INCLUSIONS IN STEEL WITH A HIGH AL CONTENT AND CASTING TEMPERATURE AFTER CORROSION TESTS IN CARBON FREE AND CONTAINING REFRACTORIES

Jens Fruhstorfer[1]*, Steffen Dudczig[1], Leandro Schöttler[2], Christos G. Aneziris[1]
[1]Institute of Ceramic, Glass and Construction Materials, Freiberg, Germany,
[2]Deutsche Edelstahlwerke GmbH, Siegen, Germany

ABSTRACT

During the remelting tests, the carbon free crucibles corroded whereas the carbon containing crucibles were negligibly attacked. On the carbon containing crucibles inclusions attached. This study analyzed melt oxygen contents, interface properties and steel compositions with their inclusions to investigate the mechanisms of inclusion formation and deposition.

The melt and steel oxygen contents were higher for the tests in the carbon free crucibles. Into these crucibles, the deoxidants Mn and Si diffused. Reducing the deoxidant content gave higher O levels in the steel and less inclusions, mainly SiO_2-core–MnS-shell ones. The amount of inclusions in the steel was highest after remelting in a carbon and nanoadditives containing crucible with a Zr and Ti doped alumina (AZT) graining. The inclusion amount decreased with increasing melting time due to deposition on the refractory surface for all inclusion types. The Ti from the AZT and the nanoadditives supported inclusion growth and deposition.

For less inclusions, mullite and for capturing inclusions, carbon bonded AZT with nanoadditives shows a high potential.

Keywords: Clogging, MnS, Erosion, Corrosion, Deposition

INTRODUCTION

Increasing steel quality requirements are met by reducing non-metallic inclusions impairing the mechanical steel properties[1].

Non-metallic inclusions are avoided or removed by chemical or physical refining, respectively. Physical refining (filtration) is performed by either surface or deep bed filtration. During deep bed filtration, the melt flows through the filter and inclusions are entrapped on the filter surface. The efficiency of deep bed filters improves with increasing residence time of the melt in the filter and with increasing inclusion size[2;3].

The inclusions are transported to the filter surface by the melt flow. The deposited inclusions sinter together and to the filter surface. The inclusions attach only on carbon containing refractories. After melt contact, these consist of a decarburized zone with an interfacial layer on top on which the inclusions attach. Deposition increases with increasing contents of impurities[2;4].

In a previous study[1], corrosion of carbon free and containing refractory crucibles by an Al-killed steel with a high casting temperature was investigated. The refractory crucibles were Al_2O_3, mullite, Al_2O_3-C, Al_2O_3 doped with ZrO_2 and TiO_2 (AZT), AZT-C and AZT-C with nanoadditives. The carbon free refractories corroded whereas the carbon containing refractories were negligibly attacked. On the carbon and nanoadditives containing AZT crucible an interfacial layer formed on which more inclusions attached than on the other carbon containing refractory surfaces.

Pursuing the previous investigation, the present study analyzes melt oxygen contents, interface properties and steel compositions with their inclusions to investigate the mechanisms of inclusion formation and deposition. The aim is to determine significant effects influencing the refractory behavior with respect to subsequent applications as lining or filter material for steel melts.

Tab. 1: Remelting trials and crucible types (AZT – Zr and Ti doped alumina, C – carbon, n – nanoadditives)

Batch	Hold time	Bond	Nanos	Matrix
Alumina (A)	60 min	ceramic	no	A
Mullite (M)				M
AZT				AZT
A-C*		carbon	no	A
AZT-C				AZT
AZT-C-n			yes	AZT
AZT-C-n	30	carbon	yes	AZT

* Steel sample taking after 4, 12, 18, 26 min of hold time

EXPERIMENTAL

The crucibles for the corrosion experiments were prepared from castables with maximum grain sizes of 3 mm as described in a previous study[1]. Carbon free castables with matrices of alumina, mullite and alumina doped with 2.5 wt% zirconia & 2.5 wt% titania (AZT) were applied. Furthermore, castables containing carbon and alumina or AZT graining were prepared. In addition, carbon containing AZT castables with nanoadditives (in total 0.01 wt% of carbon nanotubes and alumina nanosheets) were used. The added carbon amount was 4 wt% of a modified coal tar pitch because this was the minimum carbon addition necessary to form a carbonic matrix. The castables' particle size distributions were designed according to a modified Andreasen model.

After mixing and shaping, the alumina and mullite crucibles were sintered at $1600\,^{\circ}\mathrm{C}$ for 3 h. The AZT castable was fired for 3 h at $980\,^{\circ}\mathrm{C}$ due to a low refractoriness under load. The carbon containing samples were coked at $1000\,^{\circ}\mathrm{C}$ for 5 h.

For the corrosion experiments, an application-near setup[1] in an inductively heated melting unit of a metal casting simulator was used. The refractory crucibles were filled with 20 – 25 kg of the steel 17CrNiMo7-6. To reduce the oxygen content it was twice evacuated and then flushed with argon gas to ambient pressure. Then it was heated by $\approx 250\,\mathrm{K/h}$ to the casting temperature. The conducted remelting resp. corrosion tests are listed in Table 1. About every 10 min during the hold time, the temperature and oxygen content was measured. Cooling was carefully performed under argon atmosphere to reduce the risk of cracking.

The used steel 18CrNiMo7-6 had a high casting temperature of $1580\,^{\circ}\mathrm{C}$. The steel composition was determined by spark emission spectrometry, combustion-infrared absorption and elemental analyzes. After the corrosion tests, the steel compositions were determined similarly. The samples for the steel composition measurement were taken from about half the radius of the steel in-

*Email: jens.fruhstorfer@ikgb.tu-freiberg.de

Tab. 2: Mean oxygen contents and correlation coefficients between a_O and temperature (bold – stat. significant ones)

Crucible type	$a_{O_{mean}}$ in ppm	Coefficient
A	36 ± 2	**+0.768**
M	37 ± 5	**+0.987**
AZT	53 ± 7	+0.673
A-C*	32 ± 3	+0.198; **+0.919****
AZT-C	32 ± 3	**+0.976**
AZT-C-n	29 ± 5	-0.111
AZT-C-n (30 min)	35 ± 2	**+0.980**

* Sample taking of steel after 4, 12, 18 and 26 min
** without data point after 15 min

Tab. 3: Steel compositions in wt% before & after remelting (AZT – Zr and Ti doped alumina, C – carbon, n – nanoadditives)

Batch	Si	Mn	Ti	Ca	O
New steel	0.19	0.62	<0.001	0.0008	0.0029
Alumina (A)	0.19	0.57	0.0023	0.0002	0.0028
Mullite (M)	0.22	0.57	0.0011	0.0002	0.0028
AZT	0.04	0.35	<0.001	0.0002	0.0070
A-C	0.19	0.61	<0.001	0.0002	0.0029
AZT-C	0.21	0.62	<0.001	0.0002	0.0024
AZT-C-n	0.21	0.61	0.0013	0.0002	0.0020
AZT-C-n (30 min)	0.19	0.64	<0.001	0.0001	0.0017

got. The samples for the inclusion analyses were cut out of sections 3 cm from the steel–refractory-interface. The amount and distribution as well as the chemistry of the inclusions was investigated by Aspex scanning electron microscopy (SEM) which automatically maps inclusions by their size up to $25.2\,\mu m$ and lists them in defined inclusion type classes. The defined inclusion types were Al_2O_3, Ca-Aluminate, Mg-Spinel, Al-Mn-Mg-Fe-Ca-Silicate, SiO_2, MnO/MnS, CaO/CaS, Dirt, Fe-Oxide, Scratch and Other inclusions. Additionally, the sum of all inclusion types was defined as a class.

After the corrosion tests, the surfaces of the crucibles were investigated by light microscopy for roughness determination and SEM accompanied by energy-dispersive X-ray spectrometry.

RESULTS AND DISCUSSION

Melting trials

During holding, temperatures and O contents were logged. The mean oxygen contents are shown in Table 2. It is known that higher temperatures lead to higher O contents [1]. Therefore, the correlation coefficients between the O content and temperature were determined and statistically tested, cf. Table 2. A high coefficient describes a strong linear relation.

The courses of the O contents during holding were for the AZT and carbon & nanoadditives containing AZT crucibles with a hold time of 60 min not explainable by the temperature only. Additional reactions besides solution and precipitation/evaporation occurred. During melting in the carbon bonded alumina crucible, steel samples were taken with high silica containing samplers. Removing only a single data point gave a significant correlation. Without sample taking it would presumably correlate and, thus, sample taking affects the oxygen situation.

To investigate the effects of the factors 'Matrix material', 'Bond type', 'Nanoadditives' and 'Hold time', analyses of variances (ANOVAs) were applied. An ANOVA tests means on their statistical difference. The application of the carbon bond instead of the ceramic bond led to about 9 ppm lower O contents. Due to decarburization of the carbon containing refractory surfaces, carbon dissolved into the steel and formed CO gas [4]. The effect of the matrix material was significant due to the increased oxygen content of the steel melted in the AZT crucible. The nanoadditives did not affect the O content. Nevertheless, the oxygen contents decreased significantly with increasing hold time. Possible reasons are the formation of CO gas or precipitation of deoxidation inclusions.

Steel compositions and inclusion analyses

The relevant steel compositions are given in Table 3. Furthermore, Al had a content of 0.022 wt% before remelting and after remelting contents <0.001 wt% independent on the crucible type.

Firstly, correlation analyses were performed to determine groups of elements acting together or similarly. Two groups were found. One was Al–Ca with a strongly positive correlation (coefficient 0.987). Another was O–(Si,Mn), where increasing Si and Mn values strongly linear correlated with decreasing O contents (coefficients ≈ -0.96). Si also correlated negatively with the final melt oxygen content of the hold time. Mn showed the tendency to correlate negatively with the mean oxygen content (Table 2). The remaining element Ti did belong to a group.

Followingly, it was investigated by ANOVAs if there were differences between the steel compositions before and after remelting, depending on remelting time or on the refractory (considering the 'Matrix material', 'Bond type' and the 'Nanoadditives'). The addition of nanoadditives did not affect the steel compositions.

The group Al–Ca showed significant differences before and after remelting, cf. Figure 1(a), but not depending on the refractory material. Calcium modifies alumina inclusion shapes, forming globular calcium aluminate inclusions [3].

The group (Si,Mn)–O was influenced by the refractory material, cf. Figure 1(b). Mn and Si easily diffused into the refractories and formed manganese aluminates and manganese aluminosilicates [1]. Consequently, for the carbon free systems, especially if strong corrosion occurred, high contents of the deoxidizers diffused into the refractories. Reducing their amounts in the steel led to increasing oxygen contents, which explains the negative correlations.

Ti was affected by the refractory material, cf. Figure 1(c). It diffused from the AZT containing materials into the steel [1]. The oversaturation of Ti in these melts led to the precipitation of Ti containing inclusions.

As for the steel compositions, the inclusion types were tested for grouped behavior but also to resolve misclassifications. Two main groups, one containing subgroups, were determined.

The first group comprised the defined inclusion types Al_2O_3–Ca-Aluminate–CaO/CaS in line with the Ca–Al group from the steel compositions. The correlations were all positive, however, between Al_2O_3 and Ca-Aluminate only a low linearity (coefficient 0.42) indicated that an interaction occurred. The group corresponds to calcium aluminate and remaining alumina inclusions.

The second group was Sum-of-types–(MnO/MnS–Scratches, SiO_2–Fe-Oxide–Other, Al-Mn-Mg-Fe-Ca-Silicate). They all had in common the Sum of types class showing that this second main group contained most of the inclusions. The majority of inclusions were MnS-shell–SiO_2-core inclusions partly with Al and Ti additions in the core. One subgroup contained MnO/MnS and Scratches corresponding to MnS with low or no SiO_2. This were no core–shell structures but remaining MnS inclusions. Another subgroup contained SiO_2, Fe-Oxide and Other inclusion types corresponding to the core–shell structures with no additional Al and Ti. The structures with Ti and Al were classified into the Al-Mn-Mg-Fe-Ca-Silicate subgroup. For the complete secound group, the correlations had low or medium linearities with coefficients be-

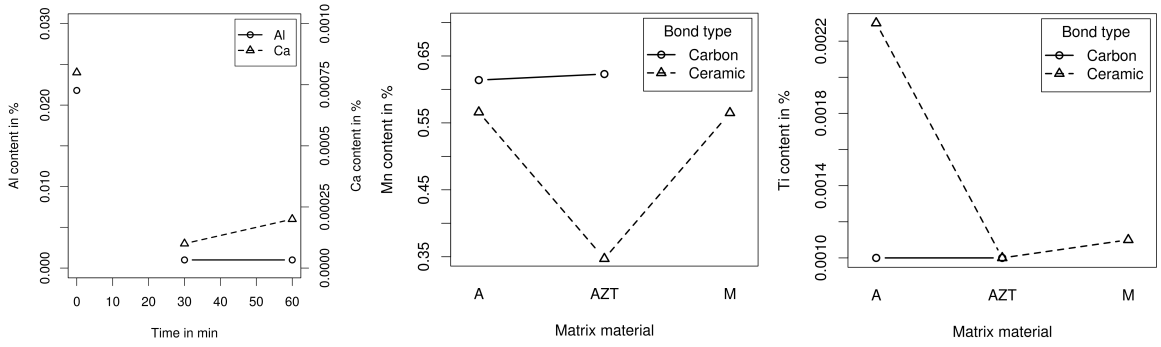

(a) Al-Ca time dependency (b) Mn interaction plot (c) Ti interaction plot

Fig. 1: Figures characterizing Ti and the groups Al-Ca and (Mn,Si)-O (A – alumina, AZT – Zr and Ti doped alumina, M – mullite)

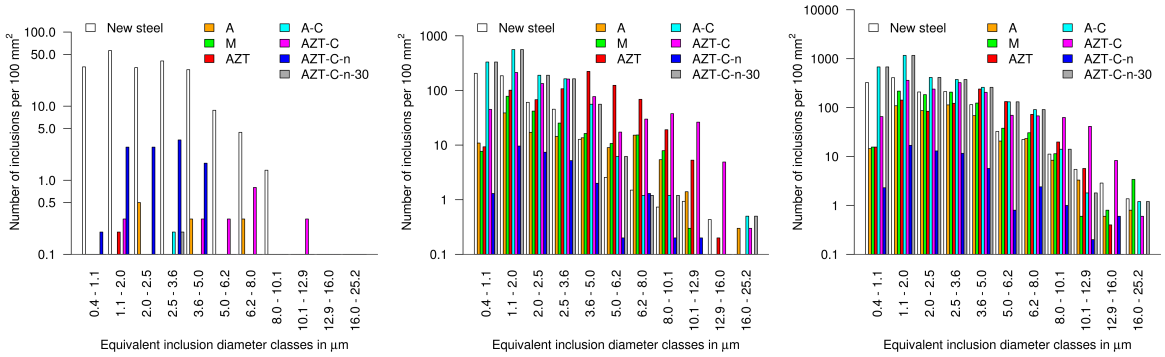

(a) Al2O3 (b) Other (c) Sums of all inclusion types

Fig. 2: Inclusion amounts dependent on inclusion size class and steel batch (before remelting – new steel, after remelting in refractory crucibles with A – alumina, M – mullite, AZT – Zr and Ti doped A, C – carbon, n – nanoadditives and 30 – 30 min hold time)

tween 0.36 and 0.71 indicating interactions which are supposedly for both main groups related to inclusion size effects.

Subsequently, ANOVAs were conducted to investigate if there were differences in the inclusion type evolution dependent on the batch and inclusion size class. Furthermore, the effects of the 'Matrix material', 'Bond type', 'Nanoadditives', 'Hold time' and their interactions were regarded. In addition, Tukey tests were used to reveal statistically differing pairs of the pairwise comparisons.

The inclusion number of the alumina and calcium aluminate inclusion group dropped significantly from before to after remelting, cf. Figure 2(a). The particles containing inclusion types Al_2O_3 and CaO/CaS had mainly sizes of 2.5–5.0 µm. The calcium aluminates were larger (6.2–12.9 µm). This explains the interactions causing the reduced linearities found by the correlation tests. There were more inclusions in the steel samples melted in the carbon bonded and AZT containing crucibles. The nanoadditives showed the tendency to decrease the inclusion amounts.

The other main inclusion group was connected by the inclusion class Sum of types (Figure 2(c)). The Tukey test revealed that the batches A-C, AZT-C and AZT-C-n (30 min) had increased inclusion amounts and that AZT-C-n (60 min) had the fewest inclusions which can be also seen in the figure. Most inclusion sizes were 2.5–8.0 µm. The addition of nanoadditives led to decreasing inclusion amounts. Supposedly, the nanoadditives led to a faster dissolution (e.g. of Ti) due to an increased reactivity and then also to a faster inclusion growth and deposition. The inclusion amounts decreased with increasing remelting time from 30 to 60 min—the inclusions had more time to grow and deposit.

The subgroup with the MnS inclusions contained small inclusions (1.1–3.6 µm). The subgroup containing the MnS-SiO_2 core–shell-inclusions without additional core elements had a bimodal inclusion size distribution peaking between 0.4–2.0 µm and 2.5–6.2 µm. The inclusion type SiO_2 showed only the first peak, whereas Fe-Oxides and Others (Figure 2(b)) showed both peaks. The small SiO_2 particles were nuclei for the core–shell structures. The Al-Mn-Mg-Fe-Ca-Silicate subgroup contained comparatively large inclusions (3.6–8.0 µm). The sizes of the core–shell inclusions with and without additional elements in the core corresponded well to the sizes of the inclusions from the Sum of types class. The effects of the material and bond type were in line with the observations for the Sum of types class. Interestingly, A-C had no influence on the inclusion type Other (Figure 2(b)). In this subgroup it was mainly connected to the SiO_2 inclusions and not to the core–shell structures. The high silica sample takers corroded and by this introduced Si into the melt which acted as nuclei for the SiO_2-core–MnS-shell inclusions. As sample taking did not influence the inclusion type Other, this is shown in Figure 2(b). For the Other inclusions, the inclusion amounts were high for AZT as well as carbon bonded crucibles.

Finally, the inclusion types and sizes were matched with the melt and steel properties. As expected, the alumina and calcium aluminate inclusions correlated with the steel elements Al and Ca for all inclusion size classes strongly linear with all positive coefficients above 0.97. For the MnS-rich, SiO_2-rich and MnS–SiO_2 inclusions, surprisingly, more Ti is related to larger inclusions (8 to 16 µm) with coefficients of 0.97. In this large size classes, most inclusions were detected in the steels melted in the AZT and AZT-C crucibles, cf. Figure 2(c). The Ti diffused firstly into the steel but then precipitated and supported inclusion growth and deposition on the refractory surfaces. This led also to the decreasing

Tab. 4: Roughness and corrosion depth (partly from prev. study [1])

Batch	ptv in mm	Total corr. depth in mm
Alumina (A)	2.70 ± 1.20	6.20 ± 0.70
Mullite (M)	1.26 ± 1.14	1.26 ± 1.14
AZT	3.55 ± 0.12	13.55 ± 0.62
A-C*	0.25 ± 0.16	0.25 ± 0.16
AZT-C	0.28 ± 0.18	0.28 ± 0.18
AZT-C-n (60 min)	0.53 ± 0.39	0.53 ± 0.39
AZT-C-n (30 min)	0.22 ± 0.14	0.22 ± 0.14

* peak–to–valley = max. height difference of surface profile
** Sample taking after 4, 12, 18 and 26 min of holding time

values of Ti in the AZT containing steel samples. In the inclusion type Other, for inclusion sizes between 5.0 and 6.2 µ, Si and Mn showed negative coefficients (-0.96) and O a positive one (0.96). In Figure 1(b) can be seen that Mn and equivalently Si contents were very low for the steel melted in the AZT crucible. And for this batch also the inclusion amount of the type Other peaked between 5.0–6.2 µ, cf. Figure 2(b).

Refractory surface analyses

In previous studies [1], the refractory surfaces including the roughness by the peak–to–valley (ptv) parameter as well as the total corrosion depth were analyzed.

The ANOVAs returned, that the carbon bonded systems had low roughnesses whereas mainly alumina and AZT had increased ones. The nanoadditives showed no influence. The total corrosion was influenced by the 'Matrix material', 'Bond type' and their interaction. The carbon bonded materials were negligibly corroded. The carbon free AZT was strongest corroded. Interestingly the mullite was only slightly more corroded than the carbon bonded systems [1]. With increasing hold time from 30 to 60 min, the tendency that the roughness increases became apparent for the AZT-C-n crucibles. The deoxidation inclusions formed in the melt, grew there and were moved to the refractory surface where they attached. In Figures 3(b) and 3(c) can be observed that the inclusion or cluster sizes are not increasing, but just the amount. This underlines that the inclusion origin is in the melt. Furthermore, it can be seen that in the AZT-C crucible after 60 min a surface state similar the one of the AZT-C-n crucible after 30 min is observable. The Ti and the nanoscaled additives contributed, thus, notably to the kinetics.

Subsequently, the correlation coefficients were analyzed. Erosion and total corrosion correlated strongly linear with a coefficient of 0.95. The total corrosion depth furthermore correlated strongly linear positive with the oxygen content of the steel with coefficient of 0.92. From the steel compositions, additionally, only Mn and Si showed correlations, all strongly linear negative (coefficients -0.91 for Si and -0.95 for Mn). Increasing oxygen contents in the melt increased the total corrosion whereas decreasing amounts of Si and Mn in the melt increased the corrosion.

Decreasing contents of inclusion-forming elements and consequently of inclusions themselves led to increased corrosion. Thus, the diffusion of Mn and Si into the refractory leads to decreasing amounts of these deoxidizers in the steel. Oxygen contents remain increased but simultaneously also deoxidation inclusions decrease. To these also the SiO_2 nuclei of the MnS-SiO_2 inclusions count.

The detached layer in Figure 3(c) contained besides Al and O also Si, Ca, Mg and partly Ti. In line with Poirier and Thillou [4], a vitreous layer formed. As it appeared only for the most reactive system with the nanoadditives and a long hold time of 60 min, also here the kinetics are essential.

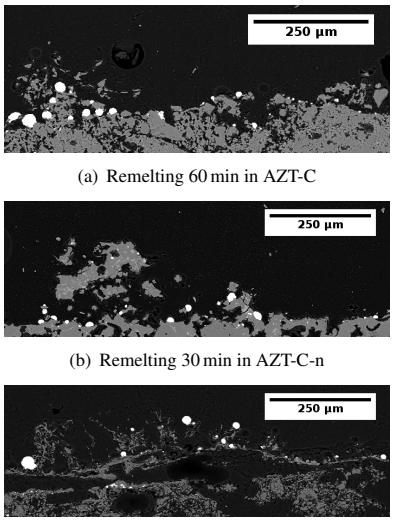

(a) Remelting 60 min in AZT-C

(b) Remelting 30 min in AZT-C-n

(c) Remelting 60 min in AZT-C-n

Fig. 3: SEM images of crucible surface sections

CONCLUSION

The melt and steel oxygen contents were higher for the tests in the carbon free crucibles. Into these crucibles, the deoxidants Mn and Si diffused. Reducing the deoxidant content gave higher oxygen levels in the steel and less inclusions of mainly SiO_2-core–MnS-shell inclusions. The amount of inclusions in the steel was highest after remelting in a carbon and nanoadditives containing crucible with a Zr and Ti doped alumina (AZT) graining. The inclusion amount decreased with increasing melting time due to deposition on the refractory surface. The Ti from the AZT and the nanoadditives supported inclusion growth and fastened the deposition. The amount of alumina and calcium aluminate inclusions generally decreased with remelting.

For less inclusions, mullite and for capturing inclusions, carbon bonded AZT with nanoadditives shows a high potential.

ACKNOWLEDGEMENT

The authors thank the German Research Foundation (DFG) for supporting this study in the subproject C01 of the CRC (SFB) 920.

REFERENCES

[1] J. Fruhstorfer, S. Dudczig, P. Gehre, G. Schmidt, N. Brachhold, L. Schöttler, and C.G. Aneziris. Corrosion of carbon free and bonded refractories for application in steel ingot casting. steel research international, 87(8):1014–23, 2016.

[2] S. Ali, D. Apelian, and R. Mutharasan. Refining of aluminum and steel melts by the use of multi-cellular extruded ceramic filters. Canadian Metallurgical Querterly, 24(4):311–8, 1985.

[3] Sunday Abraham, Rick Bodnar, and Justin Raines. Inclusion engineering and the metallurgy of calcium treatment. Iron & Steel Technology, July:57–68, 2014.

[4] J. Poirier and B. Thillou. Contribution of the refractory material of submerged nozzles to clogging. Stahl und Eisen, Special Issue publishing Proceedings of 37th Int. Colloquium on Refractories:114–8, Oct 1994.